Entropy and Speed: Effects of Obstacle Motion Properties on Avoidance Behavior in Virtual Environment

Yuliya Patotskaya, Ludovic Hoyet, Katja Zibrek, Julien Pettre

Entropy and Speed: Effects of Obstacle Motion Properties on Avoidance Behaviour in Virtual Reality

Yuliya Patotskaya
Inria, Univ Rennes, CNRS, IRISA
France
yuliya.patotskaya@inria.fr

Ludovic Hoyet
Inria, Univ Rennes, CNRS, IRISA
France
ludovic.hoyet@inria.fr

Katja Zibrek
Inria, Univ Rennes, CNRS, IRISA
France
katja.zibrek@inria.fr

Julien Pettré
Inria, Univ Rennes, CNRS, IRISA
France
julien.pettre@inria.fr

Figure 1: VR scene. Participants traversed a virtual room, avoiding a moving cylinder with varying speed and entropy.

Abstract

Avoiding moving obstacles in immersive environments requires adjustments in the walking trajectory and depends on the type of obstacle movement. Previous research studied the impact of speed and direction of motion but not much is known about how predictability of motion impacts human circumvention in terms of distance to the obstacle (proximity). In this paper, we investigate how participants navigate through VR collision avoidance scenarios with obstacles of varying motion characteristics in terms of speed and predictability. We introduce a novel concept of creating unpredictable motion using entropy calculations. We anticipated that higher entropy would increase the proximity distance which we measured with several metrics related to the distance from the obstacle and centre of the scene. We found a significant influence of motion speed and predictability on proximity-related metrics, with participants exhibiting a tendency to maintain larger distances in scenarios where obstacle speed and entropy were higher. We also outline two decision-making strategies for avoidance behaviour and investigate the factors that influence individuals' selection of one strategy over the other.

CCS Concepts

• **Computing methodologies** → **Perception**; **Virtual reality**; *Animation*.

Keywords

perception, obstacle avoidance, trajectory analysis, VR

ACM Reference Format:
Yuliya Patotskaya, Ludovic Hoyet, Katja Zibrek, and Julien Pettré. 2024. Entropy and Speed: Effects of Obstacle Motion Properties on Avoidance Behaviour in Virtual Reality. In *ACM Symposium on Applied Perception 2024 (SAP '24), August 30–31, 2024, Dublin, Ireland*. ACM, New York, NY, USA, 12 pages. https://doi.org/10.1145/3675231.3675236

1 Introduction

The escalating prevalence of everyday exposure to virtual environments underscores the imperative to comprehensively investigate their impact on individuals' perceptual experiences and behavioural responses within virtual worlds. In particular, as users can move through the VR scene, explore objects or meet and interact with agents, understanding how to effectively avoid such dynamic obstacles is crucial for achieving collision-free path planning. Despite a multitude of insights on how humans navigate dynamic environments [Berton et al. 2020, 2019; Bruneau and Pettré 2015; Rios and Pelechano 2020; Wolinski et al. 2014; Yin et al. 2024] and efforts to develop collision-free path planning strategies for autonomous agents [Dutra et al. 2017; Helbing and Molnar 1998; Karamouzas et al. 2014; Ondrej et al. 2010; van den Berg et al. 2011], we are still far from fully understanding these complex avoidance behaviours.

Examining predictability, which also relates to complexity and variance, is important when introducing natural and believable motions of virtual characters. Studies have explored how unpredictable agent movement affects avoidance behaviours [Lee et al. 2018]. Autonomous agents with randomized behavioural decisions mimic

, *15.00*

human unpredictability [Chittaro and Serra 2004]. Adjusting animation speed, joint rotations and predictability can also create natural variations in personality behaviours for virtual agents [Durupinar et al. 2016; Patotskaya et al. 2023; Souza Silva et al. 2018].

This paper presents findings regarding the influence of motion predictability on individuals' adjustment of their behaviour within a dynamic 3D obstacle avoidance scenario (see Figure 1). To design an obstacle trajectory, we employed a Wiener process-based model, affording partial control over both predictability and speed of motion. Additionally, we outline a methodology for quantifying predictability using Sample Entropy (SampEn). Within the framework of our experimental design and user data analysis, our central question is: How do individuals adapt their locomotion in response to varying obstacle speed and predictability levels?

The primary objective of this experimental study is, therefore, to investigate the influence of the entropy of the obstacle motion on human perception within the context of Virtual Reality (VR). The main contributions of this paper are: a) insights into how participants modulate their responses in relation to key properties of obstacle motion, such as speed and predictability, in dynamic environments; b) outlining two distinctive circumvention strategies: "avoiders" and "anticipators", and conclude on their relation to obstacle motion properties; c) providing objective metrics and approaches for the analysis of participant's experience, obtained by integrating user strategy analysis, trajectory analysis and, in particular, proximity metrics; d) providing a paradigm to synthesize the motion with a semi-controlled randomness and e) establishing a methodology of entropy computation in relation to the avoidance measure to obtain a quantitative representation of the relationship between avoidance and predictability.

2 Related Work

2.1 Perception of Motion Properties

Investigating motion predictability and speed is of paramount importance in simulation and animation domains. Considering the research done on motion predictability, Lee et al. [2018] showed how the participants' behaviour is influenced by different behaviours of virtual and real humans, including idle standing, jumping, and walking. They investigated potential rationales behind the differences in locomotion behaviour, emphasizing the influence of social expectations. The predictability is also accounted in modeling of gestures of virtual characters, e.g., using Perlin noise to model the neuroticism of a conversational agent [Sonlu et al. 2021]. Patotskaya et al. [2023] used less controlled and predictable gestures to model a neurotic personality of a virtual human. They found that neuroticism in gestures of virtual characters affects participants' avoidance behaviour, which may suggest that participants reacted on unpredictability in character movements itself.

In the realm of designing of natural and believable motions for virtual character animations, speed is a more commonly addressed aspect in research compared to predictability. In the frequently used OCEAN model [Goldberg 1992] neuroticism is often associated with speed [Chittaro and Serra 2004]. Early works [Brebner 1985; Lippa 1998] found differences between introverts and extroverts in speed and frequency of movements, findings which have also been corroborated in the context of virtual agent motion [Neff et al. 2011, 2010]. The latter research incorporated an approach to manipulate timing, which also relates to speed, aiming to achieve a controllable perception of emotional stability in virtual agents. The research of Durupinar et al. [2016] based on the EMOTE system [Chi et al. 2000] involved modifying the speed of an animation in a non-uniform manner to implement Time Effort of Laban Movement Analysis [Laban 1950] (LMA) in a natural way. Alaoui et al. [2017] computed Flow Effort of LMA via approximation by the shapes of speed and energy curves, while Garcia and Ronfard [2020] demonstrated the significance of natural motion descriptors such as equi-affine speed and acceleration in Laban Effort recognition tasks.

We also briefly reference notable studies of Vesper et al. [2011] and Glowinski et al. [2013] demonstrating that individuals can adapt their behaviour to change or maintain their predictability in specific social contexts. This serves as an additional motivation to study motion predictability and develop a technical foundation for it, targeting understanding of more advanced motion and behaviour properties of virtual and real humans.

Our research is inaugural in addressing the impact of motion predictability itself, while also advancing our comprehension of the effects of obstacle speed on human behaviour and perception within avoidance scenarios.

2.2 Behavioural Measures in VR

Locomotion-based experiments involving collision avoidance of virtual entities, obstacles, or characters in VR [Berton et al. 2019; Bruneau and Pettré 2015; Cutting et al. 1995; Darekar et al. 2015, 2017; Lynch et al. 2018], are extensively employed due to the rich information contained in participants' trajectories. These trajectories offer valuable insights into individuals' experiences while performing everyday tasks encountered in physical reality. Investigating the avoidance and maintenance of personal space around virtual characters provides insights into how individuals navigate social situations [Bourgaize et al. 2021; Mousas et al. 2021; Nelson et al. 2023], reflected in metrics like trajectory length, average curvature, maximal deviation, and clearance distance. Similarly, Darekar et al. [2015; 2017] measured dynamic clearance (DC) and instantaneous distance from obstacle at crossing (IDC). It is also shown that clearance distance [Argelaguet-Sanz et al. 2015; Souza Silva et al. 2018] and critical point [Hackney et al. 2015] changes when participants avoid virtual humans and virtual obstacles. Lee et al. [2018] showed changes in walking speed, observation ratio, clearance distances, and head movements, when avoiding a moving obstacle. However, the avoidance was shorter when passing repetitive behaviour. Cinelli and Patla [2008] studied if participants are changing their walking speed and heading in a consistent manner independently of the spatial constraint location and object's approach speed. In their studies, Olivier et al. [2012] investigated collision avoidance between two walkers and proposed a minimum predicted distance (MPD) to predict collision risk, which was further referenced in VR studies [Darekar et al. 2018]. Unrestricted trajectories generated during virtual walking can be analyzed geometrically and temporally, with metrics such as task completion time, distance traveled, and number of collisions [Cirio et al. 2013]. Perrinet et al. [2013] proposed metrics including walking speed, interpersonal distances, and relative positions of real and virtual

humans. Recent studies suggested more detailed participants' trajectory analyses by calculation of a deviation point [Bourgaize et al. 2021] and turning point [Patotskaya et al. 2023].

A distinct line of research endeavour to capture specific locomotion adaptations and locomotory patterns demonstrated by participants [Bönsch et al. 2016; Hackney et al. 2018; Podkosova and Kaufmann 2018; Snyder et al. 2022]. The participant's selection of the optimal strategy in each situation influences the types of locomotion adjustments, thereby affecting both walking direction and speed [Fajen and Warren 2003]. Fajen and Warren [2004] and a subsequent study by Cinelli et al. [2008] classified the participant strategies for reaching a target, identifying two predominant approaches: pursuit or interception. The recognition and integration of variations in avoidance strategies are essential in the design of autonomous agents in simulations, wherein agents possess the flexibility to adapt their speeds or orientations, to effectively execute collision avoidance maneuvers [Dutra et al. 2017; Helbing and Molnar 1998; Jovancevic-Misic and Hayhoe 2009; Karamouzas et al. 2014; Ondrej et al. 2010; van den Berg et al. 2011; Zeng and Bone 2012]. In summary, the investigation of strategies plays a pivotal role in understanding human locomotion adaptations and patterns, assessing user performance in VR.

Within the scope of VR experience evolution paradigms, we focus on a goal-oriented locomotion scenario with obstacle avoidance, analysing user behavioural responses using metrics derived from their trajectories.

3 Experiment

We selected a scenario in which participants navigated through a virtual room, strategically avoiding a dynamic obstacle animated with different levels of predictability (i.e., entropy), within a spatial environment conducive to circumvention.

In particular, we are outlining the following hypotheses:

H1: There is a direct relationship between the entropy of obstacle motion and metrics related to preserved personal space. Specifically, we predict that as the entropy of obstacle motion increases, individuals will exhibit a significantly greater avoidance distance.

H2: The speed of obstacle motion affects metrics related to preserved personal space. We suppose that the higher the speed of the obstacle the higher avoidance distance.

H3: Individuals use various strategies for obstacle avoidance. The choice of strategy impacts participants' proximity across Conditions characterized by different speed and entropy levels.

3.1 Stimuli Creation

As mentioned in Section 1, our primary objective is to investigate the influence of the predictability of obstacle motion on human perception within VR contexts.

Prior to our experiment, our objective was to generate signals (i.e., motion trajectories) with controlled variations of their characteristics, such as speed and predictability. To this end, we chose a Wiener process (which produces continuous trajectories with partially controlled randomness), described using a Geometric Brownian Motion equation, capturing both the deterministic motion drifts, represented with heavy-tailed distribution [Niu et al. 2021] and the stochastic fluctuations inherent in its dynamics [Capasso and Bakstein 2015; Kosowski and Neftci 2015]. By direct integration of the Geometric Brownian Motion equation we obtain the lateral obstacle displacement $S(t)$ from scene center at time t:

$$S(t) = S(0) \cdot e^{(\mu - \frac{\sigma^2}{2})t + \sigma W(t)}$$

where $S(0)$ is the initial obstacle position, $W(t)$ is the Wiener process representing random fluctuations, μ is the expected rate of change and σ is the randomness in obstacle displacement. We systematically varied μ and σ to generate a multitude of signals which represented the motion trajectories. We then empirically evaluated the trajectories in a pilot study and selected those that exhibited the desired range of visual unpredictability, were easily discernible for users studies, and conformed to specified speed categories.

In order to create control conditions in the form of predictable motion for comparison purposes, we also created sinusoidal signals of both slow and fast speeds (see Figure 2). We added Gaussian noise ($\sigma = 2$) to generate two more obstacle trajectories, which served to studying how noise affects users' avoidance patterns and to increase obstacle speed while maintaining a visually reasonable motion as sinusoidal oscillations beyond 1 Hz become unnatural.

Following the two strategies described above, we generated a collection of ten 10-s spatio-temporal signals, sampled at 40 Hz, representing variations in both speed and entropy (Figure 2). Finally, each obstacle trajectory was scaled (by a factor of 2) as to ensure a total motion displacement within a 1m-radius from the center of the virtual scene. The obstacle moved laterally perpendicular to the observer's path within the scene. Obstacle speeds range from 1.2 m/s to 4.9 m/s across different levels, aligning with human walking [Bohannon 1997; Nelson et al. 2023] and running [Selinger et al. 2022] speeds, which would facilitate future exploration of virtual human movements and locomotion properties.

For the naming of the levels, we employ the following convention: 'P' denotes periodic and 'Sto' - stochastic. For periodic conditions, 'LF' signifies low frequency, 'HF' - high frequency, and 'N' indicates the addition of Gaussian noise. The decimal number represents the average speed of the obstacle in m/s.

3.2 Apparatus & Task

Participants were immersed into the VE (implemented in Unreal Engine, v. 5.0.1) using a HTC Vive Pro head mounted display with a Vive Wireless adapter, and HTC Vive controllers. They saw a virtual scene displaying a moving virtual entity (cylinder diameter of 50 cm), as well as the controllers with realistic virtual hands attached to them, as a reference of their body in the VE. They were instructed to traverse the virtual scene from one specified target A to B located on the opposite side (denoted by green crosses, see Figure 1 and 3), while avoiding collisions with the virtual obstacle (if present). The trial ended upon reaching target B, and a new trial was initiated starting from target B towards A. This process was repeated multiple times until completion of the experiment. Participants started each trial positioned in front of virtual doors (Figure 1, left), to open which, they were required to stand at the center of the green cross and gaze straight ahead for 0.25 s. Once the doors opened, participants had the autonomy to start walking.

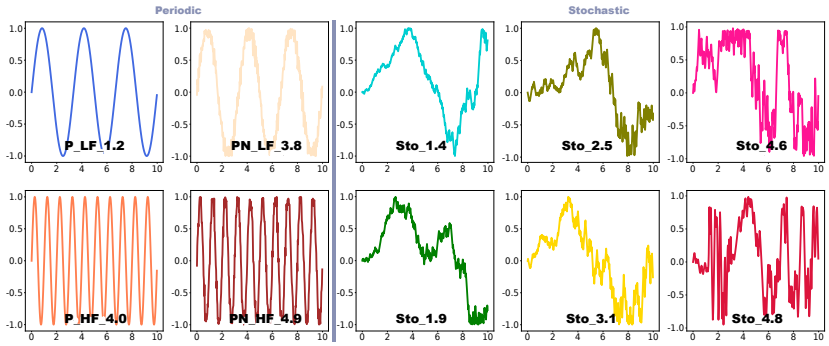

Level ID	Signal properties	Avg Speed (m/s)	Speed SD (m/s)
Empty	No obstacle	-	-
Static	Static	0	0
P_LF_1.2	Periodic, Low Frequency	1,2	0,6
Sto_1.4	Stochastic, μ=1.34,σ=-0.23	1,4	0,83
Sto_1.9	Stochastic, μ=1.34,σ=0.39	1,94	0,78
Sto_2.5	Stochastic, μ=0.90,σ=-0.60	2,54	1,3
Sto_3.1	Stochastic, μ=1.18,σ=0.55	3,07	1,4
PN_LF_3.8	Periodic, Low Freq., with noise	3,75	3,05
P_HF_4.0	Periodic, High Freq	4	1,92
Sto_4.6	Stochastic, μ=1.18,σ=-1.34	4,58	2,87
Sto_4.8	Stochastic, μ=-0.71,σ=-1.5	4,75	3,43
PN_HF_4.9	Periodic, High Freq., with noise	4,9	3,81

Figure 2: Signals used for obstacle motion animation ordered in increasing average speed: periodic group (left) and stochastic group (right); x-axis: time (s), y-axis: lateral displacement from center (m). Table of signals' main characteristics: stochastic (with specified μ and σ used for Wiener process) or periodic; average speed and standard deviation (SD) of obstacle.

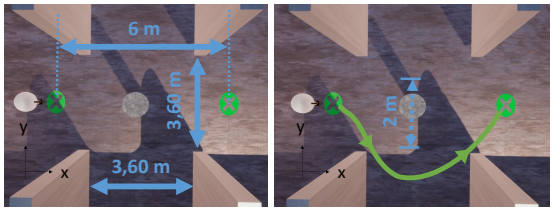

Figure 3: Top view of the VE: 1) Scene configuration; 2) Obstacle displacement and example participant trajectory.

3.3 Experimental Design

As described above, we designed 12 conditions: 1 empty scene without an obstacle, 1 with a static cylinder, and 10 conditions involving a moving cylinder. To mitigate potential biases in user trajectories within the VE, we imposed specific constraints on the configuration of the virtual room (Figure 3). Walls were positioned at a considerable distance from the user's path, and passages were limited to 3.6 m. The experimental setup, considering prior research findings [Aravind and Lamontagne 2014; Cinelli et al. 2009], involved a target-to-target distance of 6 m, with an obstacle positioned in the middle of the optimal trajectory within an unobstructed space.

We opted for 3 repetitions per condition, arranged in 3 separate blocks, with one repetition of each condition in each block, presented randomly. Participants therefore performed a total of 36 trials: 12 Conditions × 3 Repetitions. The duration of the experiment was ~18 minutes. Before the experiment, participants provided their gender, age, as well as their experience with VR and we measured their height and shoulder size. They filled in a post-questionnaire where we inquired about the moving entities observed and participants' feeling of presence in the VE.

3.4 Participants

Twenty-one participants took part in our experiment (9 male, 12 females), with an average (± SD) age of 28 ± 7 years. 8 participants reported a high level of familiarity and experience with VR, 7 - medium, 6 - no prior exposure to VR. All the participants willingly participated in the study and provided informed consent.

Exclusion Criteria. Post-experiment discussions revealed that one participant with no experience with VR misunderstood the task, and perceived it as a game to deceive a moving object.

4 Analysis

The metrics we captured can be divided into categories: a) metrics related to the center of the scene (Section 4.1), b) metrics related to the center of mass of the obstacle (Section 4.2), and c) general metrics (Section 4.3). We additionally provide an approach to classify the participants trajectories according their avoidance strategy in Section 4.4. In Section 4.5, we propose a method to quantify obstacle motion predictability using Sample Entropy. As a preliminary step, we temporally resampled participants' trajectories at 40 Hz to ensure a fixed timestep.

4.1 Metrics Relative to the Center of the Scene

These metrics are related to the distance from the center of the scene, $(x, y) = (0, 0)$, and quantify the degree to which a participant deviated from the optimal trajectory in an ideal environment.

Average Distance from the center of the scene (m) is the average of Euclidean distances from partial trajectory points bounded with vertical lines $x = -1.2\ m$ to $x = 1.2\ m$ to the scene center ($\tilde{d_{SC}}$ in Figure 7, top) [Argelaguet-Sanz et al. 2015; Patotskaya et al. 2023].

Clearance Distance from the center of the scene (m) is an Euclidean distance from the scene center to the nearest point along the user's trajectory [Gérin-Lajoie et al. 2005; Sannier et al. 2023].

Maximum Lateral Deviation from the center of the scene (m) measures how far a participant's trajectory deviates laterally from the ideal path, represented by the line connecting the start and end points of the task (marked with green crosses in the VR scene).

Side-by-Side Distance from the center of the scene (m) is a lateral deviation from scene center when participant is side-by-side to the obstacle ($d_{SC}|_{x=0}$ in Figure 7, center) [Nelson et al. 2023].

4.2 Metrics Relative to the Obstacle

These metrics are related to the distance to the center of the obstacle. We applied a Gaussian filter ($\sigma = 1$) to the obstacle displacement, ensuring that the metrics reflect the overall participant movement rather than noise introduced by the obstacles.

Average Distance to the center of mass of the obstacle (m) is computed on a partial trajectory ($x = -1.2\ m$ to $x = 1.2\ m$), similar to dynamic clearance [Darekar et al. 2015, 2017; Perrinet et al. 2013], as an average of the Euclidean distances from the trajectory to the center of mass of the obstacle at each frame.

Side-by-side Distance to the center of mass of the obstacle (m) is computed similarly to the instantaneous distance from obstacle at crossing [Darekar et al. 2015, 2017; Nelson et al. 2023]. We averaged the lateral distance of the participant to the center of mass of the obstacle within a 0.5 s window on crossing at the crossing of the obstacle latitude, i.e. $x = 0$ ($d_{OC}\big|_{x=0}$ in Figure 7, bottom).

4.3 General Metrics

We also analysed commonly used metrics as: a) *Travel Time (s)* – time the participant spent traveling between the two green crosses (from the start to the target) in the VE and b) *Trajectory Length (m)* – length of the walking trajectory between the start and target spots [Berton et al. 2019; Mousas et al. 2021; Patotskaya et al. 2023].

4.4 Strategies Classification

We observed, that some individuals appeared to opt for a strategy of waiting for the obstacle to clear their path before proceeding, while others chose to traverse the obstructed portion of the scene directly. This observation highlights the diversity of approaches individuals may employ when faced with obstacles, as described in previous literature on pedestrian avoidance [Fajen and Warren 2003; Huber et al. 2014] and motion strategy planning, wherein autonomous agents were programmed to adapt their speeds or angles during avoidance maneuvers [Bruneau and Pettré 2015; Dutra et al. 2017; Helbing and Molnar 1998; Karamouzas et al. 2014; Ondrej et al. 2010; van den Berg et al. 2011]. Since these strategies could impact the analysis of results, we decided to separate our data into two groups: "anticipators" (adjusting the speed while circumventing) and "avoiders" (adjusting the circumvention path).

To distinguish between these two strategies, we detect if participants significantly decelerated to wait for the obstacle to move away. First, we identify where their speed peaked along the trajectory. Then, we backtrack to where their speed dropped below 25% of its maximum, marking it as the final decision point. If the final decision point's x coordinate is over 50 cm from the starting area, it is categorized as anticipation. If 3 or more out of 10 levels with a moving obstacle, participants exhibit anticipation, we classify the repetition as anticipation; otherwise, as avoidance.

4.5 Motion Entropy

While average speed serves as a straightforward metric, the characterization of motion in terms of predictability is more challenging which we explore through the concept of entropy. First, it is important to clarify that the definition of entropy varies depending on the specific task. This led to the definition of numerous entropy metrics (e.g., Approximate Entropy [Chen et al. 2008], Distribution Entropy [Li et al. 2018], Fuzzy Entropy [Li et al. 2018], Conditional Entropy [Shi et al. 2019; Yan et al. 2022]). In this paper, we rely on Sample Entropy (SampEn), which is widely used for quantifying the predictability and complexity of time-series data in fields such as neuroscience [Bhavsar et al. 2018; Glowinski et al. 2013; Yogarajan et al. 2023], healthy physiology [Richman and Moorman 2000] or biomechanics [Gates et al. 2022; McCamley et al. 2018].

Second, the quantification of signal complexity through SampEn is contingent upon the appropriate selection of two parameters: m (embedding dimension), which corresponds to the length of the sequences to be compared, and r (tolerance), which represents the sequences' similarity [Montesinos et al. 2018; Yentes et al. 2018; Yogarajan et al. 2023]. While acknowledging the significance of m and r in SampEn analysis, it should be noted that the prevalent adoption of $m = 2$ and $r = 0.2$ in many studies lacks a strict rationale [Glowinski et al. 2013; Ramdani et al. 2009]. For this reason, we propose the systematic evaluation of these parameters and investigate a selection of optimal parameters for SampEn within the ranges of $r = [0.1; 0.3]$ and $m = [2; 100]$, based on values observed in the literature [Castiglioni et al. 2013; Montesinos et al. 2018; Yentes et al. 2018]. Figure 8 illustrates how strongly the values of entropy can vary depending on the parameters.

4.6 Statistical Analysis

The procedure of analysing results was the following. Where normality assumptions tested with Kolmogorov-Smirnov & Lilliefors test were satisfied, we used parametric statistical analyses to explore potential differences between conditions (paired sample T-test, repeated measures ANOVA), and used their non-parametric equivalent otherwise. Sphericity was also assessed using Mauchly's tests, and Greenhouse-Geisser adjustments to the degrees of freedom were applied when appropriate to avoid any violation of the sphericity assumption. We set the level of significance to $\alpha = 0.05$ and used the notations * (p-value < 0.05) to highlight significant differences in the figures. Results are reported as mean ± standard deviation. In case of a significant main or interaction effect, we performed pairwise comparisons using Tukey post-hoc tests. The Conditions were arranged in average speed of obstacle increase order, to monitor the progression of p-values.

Additionally, we conducted a linear regression analysis to outline the correlation between proximity to the obstacle and the entropy of the obstacle's motion (results presented in Section 5.2).

5 Results

As detailed in Section 3.1, our investigation focused on the ways in which individuals circumvent static and dynamic obstacles moving with various entropy. When referring to "metrics related to the distance to the scene center", we encompass all four metrics listed in Section 4.1 as we identified several similar statistical patterns in their analysis. We maintain consistent color codes for the levels as described on the Figure 2 for both statistical results and trajectory visualization.

5.1 Trajectory Analysis

Metrics relative to the center of the scene. For all four metrics we found a main effect of Condition with a large effect size, i.e. for Side-by-side Distance ($F_{7.2,425.9} = 178.1, p < 0.001, \eta_p^2 = 0.751$), Average Distance ($F_{4.62,90.8} = 90.8, p < 0.001, \eta_p^2 = 0.580$), Clearance Distance ($F_{11,209} = 131, p < 0.001, \eta_p^2 = 0.751$) and Maximum Lateral Deviation ($F_{4.91,93.37} = 122, p < 0.001, \eta_p^2 = 0.687$) from center of the scene. Overall, these results suggest that the factor of Conditions with different speed and entropy of the obstacle motion influenced the metrics related to the distance to the center of the scene, that is why we proceed with a Tukey post-hoc to investigate significant differences.

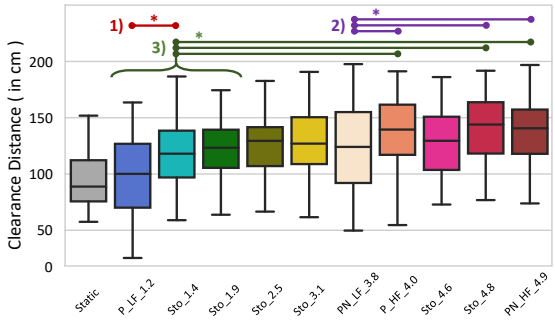

Figure 4: Clearance from scene center: key significant differences highlighted in groups 1, 2 and 3. Full Tukey post-hoc analysis provided in Table 1.

In most of the Conditions we observe that the increase of speed and entropy tends to lead to the increase in avoidance distance to the center of the scene, which validates the hypothesis H1 and H2. However the p-value analysis shows that speed increase leads to significant difference in avoidance distances within certain thresholds. In particular, we can extrapolate two general conclusions, which are adding essential clarifications to our hypothesis H2. First, for the levels with similar speeds (the average obstacle speed difference < 1 m/s), no significant differences were found in individuals' distance-related metrics. Second, for levels characterized by an average obstacle speed exceeding 3.1 m/s, no significant differences were observed within the distance to the center of the scene metrics. In particular, analyses of average distance, maximum lateral distance, clearance distance and side-by-side distance revealed no significant difference across these higher-speed scenarios. There are, however, several exceptions of these two observations, for example Level *P_LF_*1.2 and *PN_LF_*3.8, which we relate to impact of entropy (hypothesis H1), which we are discussing in Section 6.

To validate the entropy-related hypothesis H1, we further provide a comparative analysis between periodic and stochastic levels. Despite similar speeds between the periodic level *P_LF_*1.2 and the stochastic level *Sto_*1.4, the Clearance distance to the center was significantly lower ($p = 0.04$) for the former (Figure 4, group 1). Clearance distance in Level *P_LF_*1.2 exhibited a notable decrease compared to all other levels analyzed. Despite a marginal p-value of 0.052 in comparison of Level *Sto_*1.9 and Level *P_LF_*1.2, indicating a trend rather than statistical significance, participants still appeared to take a larger space when navigating around obstacle than in Level *P_LF_*1.2 (Table 1). For the other metrics such as side-by-side distance (Figure 5 and Table 3 part 1 on the left) and average distance we have noticed trends ($p = 0.052$ and $p = 0.084$ correspondingly) that the participants tend to take a larger distance to the center of the scene when the motion is less predictable in comparison with a periodic one (Table 1). These findings highlight the impact of predictability on participants' behaviours when encountering obstacles, despite comparable motion speeds, which is in line with hypothesis H1.

Exploring further the results related to hypothesis H1, we hereby highlight the Level *PN_LF_*3.8, where the obstacle followed a displacement pattern characterized by low frequencies of sinusoidal motion with added noise. Despite the high average speed of the obstacle (due to added noise), individuals exhibited distinctly lower avoidance distances compared to other levels with similar obstacle speeds. Also, for *PN_LF_*3.8 distance-related metrics were significantly lower than for *P_HF_*4.0, *Sto_*4.8, *PN_HF_*4.9 (Figure 4, group 2). Additionally, the same analysis revealed no differences in the metrics between Condition *PN_LF_*3.8 and the Conditions where the obstacle speeds were notably lower (i.e. difference in speed $>> 1m/s$), specifically Level *Sto_*1.4 and *Sto_*1.9. At the same time, it also demonstrates that the mean of all of distances metrics in Level *PN_LF_*3.8, with low frequency periodic motion with noise, is comparable to levels with lower speeds, thereby reaffirming the observation that participants approached this obstacle similarly to how they approached obstacles with slower motion speeds. This leads us to consider that speed, while important, is not the sole determining factor influencing how the participant perceives and avoids the moving object (Figure 10). This indicates that the predictability of obstacles has a significant impact, supporting hypothesis H1 and providing additional details for H2.

In levels *P_HF_*4.0, *Sto_*4.8, and *PN_HF_*4.9, all distance metrics exhibited significant differences compared to levels *P_LF_*1.2, *Sto_*1.4, and *Sto_*1.9 (Figure 4, group 3). Specifically, the distance to the center of the scene was significantly lower in slow obstacle speed levels compared to fast ones (Figure 10), aligning with and providing detailed support for speed-related hypothesis H2.

Metrics related to the distance to the dynamic obstacle. For side-by-side distance to the obstacle, the repeated measures ANOVA revealed a significant effect of the within-subjects factor ($F_{72110,116} = 116$, $p < .001$, $\eta = 0.670$). For average distance to the obstacle on partial trajectory, the repeated measures ANOVA revealed a significant effect of the within-subjects factor ($F_{31928,52.5} = 52.5$, $p < .001$, $\eta = 0.589$).

Side-by-side distance from the participant to the obstacle gave statistical significance for the levels (Table 2) as for side-by-side distance from the scene center (Table 1), but the values behave differently (Figure 10). Additionally, a significant difference (p-value = 0.048) was observed between periodic and stochastic obstacle motion at low speeds, i.e. in Conditions *Sto_*1.4 and *P_LF_*1.2. Side-by-side distance to the scene center and to the obstacle the post-hoc reveals a statistical difference for nearly the same levels. However, we do not see a progressive increase in the mean value of the distance to the obstacle with the rise of speed and entropy, as for distance to scene center metrics (e.g. Figure 4 and 5 and Table 3 part 1), which serves as additional motivation to investigate the strategies employed by individuals (Section 4.4 and 5.3).

The ANOVA analysis of the average distance to the obstacle revealed minimal differences, probably attributed to the bias introduced by the obstacle displacement.

Other results. For all the metrics ANOVA test revealed no significant effect of repetitions. A repeated measures ANOVA found no significant effect on task completion time across the 12 conditions. For the travel distance, the same test revealed a significant main effect of the factor of the obstacle speed and entropy ($F_{5.16,97.97} = 24.2, p < 0.001, \eta_p^2 = 0.459$).

For all the metrics, Tukey's post hoc analyses, revealed an absence of distinctions in participant avoidance behaviour of a static cylinder and of the one exhibiting periodic low-frequency oscillations with speed of 1.2 m/s (*P_LF_*1.2). The analysis across various

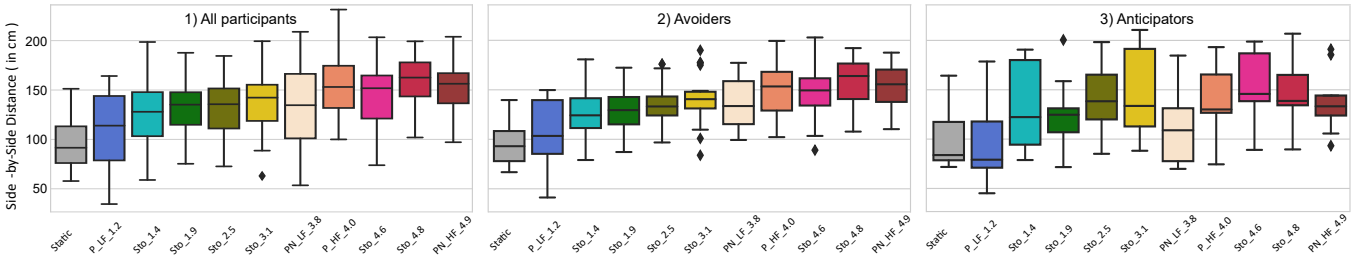

Figure 5: Comparison of side-by-side distances to the scene center for: 1) all participants, 2) "avoiders" and 3) "anticipators".

metrics indicates that participants avoided the cylinder in a similar way when it was static or periodic with low frequency.

5.2 Regression Analysis: Impact of Entropy

We conducted the linear regression analysis to find the correlation between obstacles' speed and entropy versus proximity, in particular: 1) side-by-side distance to the center, 2) side-by-side distance to the obstacle, 3) average distance to the center and 4) average distance to the obstacle. Within the range of parameters m and r, as described in Section 4.5, we computed SampEn and chose the optimal values through regression against spatial metrics. We provide a systematic evaluation of R^2 for various combinations of m and r for distance metrics in Figure 9.

The regression of entropy against side-by-side distance to the obstacle exhibits the highest coefficient of determination R^2 value of 0.8708, achieved with SampEn parameters $m = 84$ and $r = 0.1800$. The regression against the average distance to the obstacle yields a notable $R^2 = 0.8156$, attained with SampEn parameters $m = 5$ and $r = 0.2975$. When examining entropy in relation to the average distance to the center, the highest $R^2 = 0.7265$ emerges with SampEn parameters $m = 2$, $r = 0.1400$. Lastly, entropy against side-by-side distance to the center reveals an $R^2 = 0.6790$, where parameters $m = 2$, $r = 0.1375$ are found to be optimal. These results shows a strong correlation between entropy and avoidance distance.

In comparison, regression analysis showed R^2 of 0.7534 for obstacle speed versus average avoidance distance to the scene center, and an $R^2 = 0.7375$ for side-by-side distance to the scene center. However, the model poorly explains variability in obstacle distance: $R^2 = 0.5452$ for average distance and 0.0308 for side-by-side.

5.3 Strategies Classification

Within the classification strategy proposed in Section 4.4, 2 out of 20 participants were classified as "anticipators" for all 3 repetitions, while 3 of participants did so in the 2 first repetitions, and 3 only in the first repetition. The more participants became familiar with the VE, the more likely they were taking an "avoider" strategy.

The proposed classification revealed an illustrative performance on the Side-By-Side deviation from the scene center (Figure 5 and Table 3). Due to the relatively small sample size of "anticipators", we chose the non-parametric Friedman test, which yielded a significant difference ($\chi^2 = 66.8$, df = 11, $p < .001$). It is important to note that the paired comparisons (Durbin-Conover) revealed additional significant differences for the periodic levels in comparison with stochastic ones. For example, in level $P\_LF\_1.2$, the side-by-side distance was significantly lower in comparison with all the other levels which contained a dynamic obstacle. Additionally, in levels where average obstacle speed was in the range [3.1; 4.9] m/s, the distance was significantly lower in Level $PN\_LF\_3.8$, where the obstacle moved periodically with noise, versus Levels $Sto\_3.1$ and $Sto\_4.6$, where obstacle moved more randomly (p-value 0.034 and $< .001$ respectively). Side-by-side distance was also significantly lower for Level $P\_HF\_4.0$, where participants avoided an obstacle moving with high frequency periodic oscillations, than for $Sto\_4.6$, where the obstacle moved randomly ($p = 0.024$). At the same time, the difference between periodic Levels $PN\_LF\_3.8$ and $P\_HF\_4.0$ became less explicit ($p = 0.143$); however, we still observe the trend that the distance is lower in the low frequency level.

For the sets which were classified as "avoiders" the repeated measures ANOVA revealed a significant condition effect on side-by-side deviation from scene center ($F_{4.88,83.00} = 114, p < .001, \eta^2 = 0.748$) after applying the Greenhouse-Geisser correction for sphericity. Tukey test revealed fewer significant differences compared to the entire dataset. However, we still observe a consistent trend indicating that the side-by-side distance increases as the speed of the obstacle increases. These findings support our hypothesis H3, indicating that the strategy individuals employ has varying effects on distance across different Conditions (Figure 5 and Table 3).

6 Discussion

The principal finding of this study is that avoidance distance is influenced by the movement pattern of the object. Both ANOVA and regression analysis confirmed a significant correlation between entropy and speed versus proximity, which supports the hypotheses H1 and H2. In multiple conditions we observed that the increase of speed and entropy in avoidance distance to the center of the scene. This behaviour is likely associated with an anticipation of the risk of collision when a user maintains safety margins. While existing approaches for autonomous agents consider various factors, for example locomotion energy [Bruneau and Pettré 2015], interaction between individual agents [van den Berg et al. 2011], time-to-collision [Karamouzas et al. 2014], there is a distinct absence of methods that address the motion predictability of dynamic environments. Conversely, recent trends in introducing pedestrian heterogeneity in crowds [Yi et al. 2023] favor data-driven approaches [Mao et al. 2022; Xu et al. 2022]. We highlight that entropy offers the advantage of serving as an interpretable tool for quantifying motion predictability, which contributes to the long-term endeavor of realistic and reactive crowd modeling. Programming agents with an assessment of the entropy of obstacles in VEs may enhance

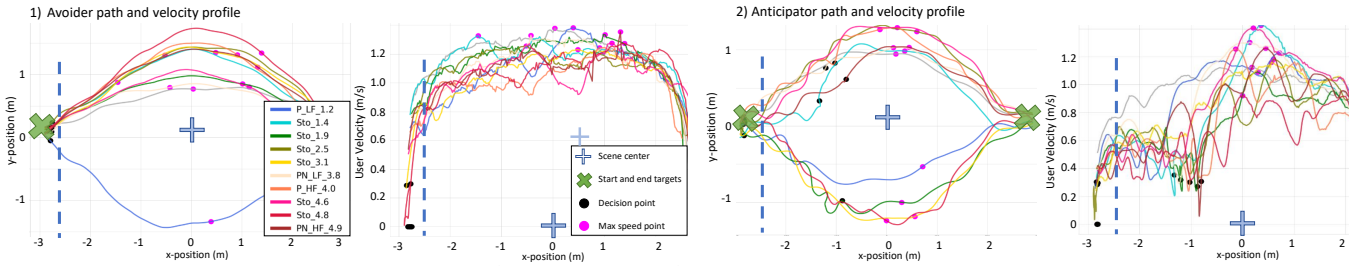

Figure 6: Examples of 1) Avoider's and 2) Anticipator's paths and speed profiles.

their natural responsiveness and introduce variance in their motions. Moreover, considering the speed and entropy of virtual agent gestures [Patotskaya et al. 2023; Sonlu et al. 2021] may contribute to determining the space required by participants to maintain a comfortable distance.

The proposed recognition and investigation of two strategies, "avoiders" and "anticipators" (see Figure 6), aligns with our hypothesis H3. This contributes knowledge to research on locomotion adaptations and walking patterns [Bönsch et al. 2016; Cinelli et al. 2008; Fajen and Warren 2004; Hackney et al. 2018; Snyder et al. 2022]. On example of side-by-side distance to the scene center, we demonstrated that "avoiders" progressively maintained greater distances as the obstacle speed increased. Conversely, "anticipators" tent to react more to obstacle entropy, preserving significantly lower distances while avoiding obstacles with periodic motion. In this experimental context, we posit that the choice of strategy is likely influenced by individuals' specifics to evaluate the collision risk [Dutra et al. 2017] and their exposure to the scene. The participants may alternate between both strategies over the experiment, with the "anticipator" being more prevalent during initial repetitions, The "avoider" strategy is more used when a participant becomes more familiar with the scene. However, the limited representation of "anticipators" in our dataset prevents us from drawing robust conclusions regarding their reaction to motion changes. Understanding of the prerequisites for different strategies could serve as valuable motivation for future investigation with a larger participant pool.

Recognizing the importance of selecting m and r in SampEn analysis, for which there is no standardized approach [Glowinski et al. 2013; Montesinos et al. 2018; Yentes et al. 2018] our goal was to identify optimal parameters for computing obstacle motion entropy that would have a stronger correlation with human reactivity. This resulted in a new endeavour: can we explain, how people perceive the motion stimuli within interpretation of the optimal parameters of entropy? Based on our results, we assume that individuals not only perceive local displacements and speed variations but also may be attentive to the global trends in obstacle motion.

In general, we did not find differences between proximity metrics between levels which displayed an obstacle moving at similar speeds (< 1 m/s difference), with several exceptions. These were the cases when the obstacle moved periodically with low frequency with and without noise applied. Participants maintained significantly shorter distances to the scene center (confirmed for all four metrics) when avoiding obstacles of periodic motions compared to stochastic (i.e., more random) ones moving at the similar speeds. At slower obstacle speeds (1.2 and 1.4 m/s), participants consistently maintained shorter distances when avoiding obstacles with periodic motion, which may signify that people are more sensitive to the predictability when perceiving the motion at lower speeds. However, when the obstacle moved with high speed (> 4 m/s) we did not find the relation between proximity and obstacle entropy.

The regression analysis suggests that measures associated with the distance between participant and obstacle itself display a notably high correlation with entropy. Metrics concerning avoidance distance between the participant and the center of the scene exhibit a strong correlation with speed and entropy, with speed demonstrating a slightly higher predictive accuracy. This finding suggests that entropy more effectively explains the proximity concerning the obstacle itself, whereas speed better accounts for the distances related to the center of the scene. We conclude that, while speed is an important factor, it is not the sole determinant influencing how participants perceive and avoid the moving object.

The proximity metrics evaluation strongly suggests that when periodic motion is complicated by noise, people's reactions to it tend to resemble reactions to periodic motion rather than to stochastic motion of the similar speed. At the same time, we admit, that individuals noticed the presence of noise in sinusoidal motions, as their avoidance distance was significantly higher.

Future work. In addition to the future research questions outlined before, we acknowledge the necessity to explore alternative methods for quantifying motion predictability beyond Sample Entropy, recognizing that it may not be the optimal or straightforward measure to characterize obstacle motion predictability. The proximity study of this experiment could potentially be enhanced by exerting stronger control over the side of the scene where the obstacle is. However in this experiment we solved this problem by introducing sufficient amount of variances in obstacle motions, randomizing the sequence of levels, and conducting repetitions, as we still see a strong effect of the proposed stimuli, speed and entropy, on proximity. We also recognize that our conclusions regarding interactions and motion properties are derived from the obstacles animated using a specific dynamic model. Extrapolating these findings on the impact of speed and entropy to other motion models, such as believable virtual humans' gestures or walking trajectories, may not be straightforward, posing a challenge for future research.

7 Conclusion

This research shows that the increase of speed and entropy of the obstacle leads to the increase in avoidance distance to the center of the obstacle motion, which validates our hypothesis. Participants consistently maintained shorter distances to the scene center when avoiding periodic motion obstacles compared to stochastic ones at similar speeds, provided the obstacle speed did not exceed 4 m/s.

The study also identified two avoidance strategies, "avoiders" and "anticipators", where "avoiders" maintain greater distances as obstacle speed increases, while "anticipators" tend to be more reactive to obstacle predictability. The preference for avoidance strategy appeared to be linked to individual participant traits rather than the movement patterns of the obstacle and may change over time as participants become more familiar with the virtual environment.

Acknowledgments

This work was sponsored by the European grant ForEVR (H2020-MSCA-IF-2020 , No. 101030793), and the French National Research Agency grant PIA program (ANR-21-ESRE-0030 CONTINUUM).

References

Sarah Fdili Alaoui, Jules Françoise, Thecla Schiphorst, Karen Studd, and Frédéric Bevilacqua. 2017. Seeing, Sensing and Recognizing Laban Movement Qualities. *Proceedings of the 2017 CHI Conference on Human Factors in Computing Systems* (2017). https://doi.org/10.1145/3025453.3025530

Gayatri Aravind and Anouk Lamontagne. 2014. Perceptual and locomotor factors affect obstacle avoidance in persons with visuospatial neglect. *Journal of NeuroEngineering and Rehabilitation* 11, 1 (2014), 38. https://doi.org/10.1186/1743-0003-11-38

Ferran Argelaguet-Sanz, Anne-Helene Olivier, Gerd Bruder, Julien Pettré, and Anatole Lécuyer. 2015. Virtual proxemics: Locomotion in the presence of obstacles in large immersive projection environments. In *2015 IEEE Virtual Reality (VR)*. 75–80. https://doi.org/10.1109/VR.2015.7223327

Florian Berton, Ludovic Hoyet, Anne-Hélène Olivier, Julien Bruneau, Olivier Le Meur, and Julien Pettré. 2020. Eye-gaze activity in crowds: impact of virtual reality and density. In *2020 IEEE Conference on Virtual Reality and 3D User Interfaces (VR)*. IEEE, 322–331. https://doi.org/10.1109/VR46266.2020.00052

Florian Berton, Anne-Hélène Olivier, Julien Bruneau, Ludovic Hoyet, and Julien Pettre. 2019. Studying Gaze Behaviour during Collision Avoidance with a Virtual Walker: Influence of the Virtual Reality Setup. 717–725. https://doi.org/10.1109/VR.2019.8798204

Ronakben Bhavsar, Na Helian, Yi Sun, Neil Davey, Tony Steffert, and David Mayor. 2018. Efficient Methods for Calculating Sample Entropy in Time Series Data Analysis. *Procedia Computer Science* 145 (2018), 97–104. https://doi.org/10.1016/j.procs.2018.11.016

R W Bohannon. 1997. Comfortable and maximum walking speed of adults aged 20-79 years: reference values and determinants. *Age and ageing* 26, 1 (1997), 15–9. https://doi.org/10.1093/ageing/26.1.15

Andrea Bönsch, Benjamin Weyers, Jonathan Wendt, Sebastian Freitag, and Torsten W. Kuhlen. 2016. Collision Avoidance in the Presence of a Virtual Agent in Small-Scale Virtual Environments. In *IEEE Symposium on 3D User Interfaces*. 145–148. https://doi.org/10.1109/3DUI.2016.7460045

Sheryl M. Bourgaize, Bradford J. McFadyen, and Michael E. Cinelli. 2021. Collision avoidance behaviours when circumventing people of different sizes in various positions and locations. *Journal of Motor Behavior* 53, 2 (2021), 166–175. https://doi.org/10.1080/00222895.2020.1742083

John Brebner. 1985. *Personality theory and movement*. Springer Netherlands, Dordrecht, 27–41. https://doi.org/10.1007/978-94-009-4912-6_2

Julien Bruneau and Julien Pettré. 2015. Energy-efficient mid-term strategies for collision avoidance in crowd simulation. In *Proceedings of the 14th ACM SIGGRAPH / Eurographics Symposium on Computer Animation* (Los Angeles, California) *(SCA '15)*. Association for Computing Machinery, New York, NY, USA, 119–127. https://doi.org/10.1145/2786784.2786804

Vincenzo Capasso and David Bakstein. 2015. *An Introduction to Continuous-Time Stochastic Processes* (3 ed.). Birkhäuser, New York, NY. https://doi.org/10.1007/978-1-4939-2757-9

Paolo Castiglioni, Sebastian żurek, Jaroslaw Piskorski, Marcin Kośmider, Przemyslaw Guzik, Emiliano Cè, Susanna Rampichini, and Giampiero Merati. 2013. Assessing Sample Entropy of physiological signals by the norm component matrix algorithm: Application on muscular signals during isometric contraction. (2013), 5053–5056. https://doi.org/10.1109/EMBC.2013.6610684

Waiting Chen, Jun Zhuang, Wangxin Yu, and Zhizhong Wang. 2008. Measuring complexity using FuzzyEn, ApEn, and SampEn. *Medical engineering and physics* 31 (07 2008), 61–8. https://doi.org/10.1016/j.medengphy.2008.04.005

Diane Chi, Monica Costa, Liwei Zhao, and Norman Badler. 2000. The EMOTE model for effort and shape. In *Proceedings of the 27th Annual Conference on Computer Graphics and Interactive Techniques (SIGGRAPH '00)*. ACM Press/Addison-Wesley Publishing Co., USA, 173–182. https://doi.org/10.1145/344779.352172

Luca Chittaro and Milena Serra. 2004. Behavioral programming of autonomous characters based on probabilistic automata and personality: Research Articles. *Comput. Animat. Virtual Worlds* 15, 3–4 (jul 2004), 319–326.

Michael E Cinelli and Aftab E Patla. 2008. Locomotor avoidance behaviours during a visually guided task involving an approaching object. *Gait & Posture* 28, 4 (Nov 2008), 596–601. https://doi.org/10.1016/j.gaitpost.2008.04.006

Michael E. Cinelli, Aftab E. Patla, and Fran Allard. 2008. Strategies used to walk through a moving aperture. *Gait and Posture* 27, 4 (2008), 595–602. https://doi.org/10.1016/j.gaitpost.2007.08.002

Michael E Cinelli, Aftab E Patla, and Fran Allard. 2009. Behaviour and gaze analyses during a goal-directed locomotor task. *Q J Exp Psychol (Hove)* 62, 3 (Mar 2009), 483–99. https://doi.org/10.1080/17470210802168583

Gabriel Cirio, Anne-Helene Olivier, Maud Marchal, and Julien Pettré. 2013. Kinematic evaluation of virtual walking trajectories. *IEEE transactions on visualization and computer graphics* 19, 4 (2013), 671–680. https://doi.org/10.1109/TVCG.2013.34

James Cutting, Peter Vishton, and Paul Braren. 1995. How we avoid collisions with stationary and moving objects. *Psychological Review* 102 (10 1995), 627–651. https://doi.org/10.1037/0033-295X.102.4.627

Anuja Darekar, Valery Goussev, Bradford J. McFadyen, Anouk Lamontagne, and Joyce Fung. 2018. Modeling spatial navigation in the presence of dynamic obstacles: a differential games approach. *Journal of Neurophysiology* 119, 3 (2018), 990–1004. https://doi.org/10.1152/jn.00857.2016

Anuja Darekar, Anouk Lamontagne, and Joyce Fung. 2015. Dynamic clearance measure to evaluate locomotor and perceptuo-motor strategies used for obstacle circumvention in a virtual environment. *Human Movement Science* 40 (2015), 359–371. https://doi.org/10.1016/j.humov.2015.01.010

Anuja Darekar, Anouk Lamontagne, and Joyce Fung. 2017. Locomotor circumvention strategies are altered by stroke: I. Obstacle clearance. *Journal of NeuroEngineering and Rehabilitation* 14, 1 (2017), 56. https://doi.org/10.1186/s12984-017-0264-8

Funda Durupinar, Mubbasir Kapadia, Susan Deutsch, Michael Neff, and Norman I. Badler. 2016. PERFORM: Perceptual Approach for Adding OCEAN Personality to Human Motion Using Laban Movement Analysis. *ACM Trans. Graph.* 36, 1, Article 6 (oct 2016), 16 pages. https://doi.org/10.1145/2983620

T. B. Dutra, R. Marques, J.B. Cavalcante-Neto, C. A. Vidal, and J. Pettré. 2017. Gradient-based steering for vision-based crowd simulation algorithms. *Computer Graphics Forum* 36, 2 (2017), 337–348. https://doi.org/10.1111/cgf.13130

Brett Fajen and William Warren. 2003. Behavioral Dynamics of Steering, Obstacle Avoidance, and Route Selection. *Journal of experimental psychology. Human perception and performance* 29 (04 2003), 343–62. https://doi.org/10.1037/0096-1523.29.2.343

Brett R Fajen and William H Warren. 2004. Visual Guidance of Intercepting a Moving Target on Foot. *Perception* 33, 6 (2004), 689–715. https://doi.org/10.1068/p5236

Maxime Garcia and Rémi Ronfard. 2020. Recognition of Laban Effort Qualities from Hand Motion *(MOCO '20)*. Association for Computing Machinery, New York, NY, USA, Article 8. https://doi.org/10.1145/3401956.3404227

Paul Gates, Franco M Discenzo, Jung Hung Kim, Zachary Lemke, James Meggitt, and Angela L Ridgel. 2022. Analysis of Movement Entropy during Community Dance Programs for People with Parkinson's Disease and Older Adults: A Cohort Study. *International Journal of Environmental Research and Public Health* 19, 2 (2022), 655. https://doi.org/10.3390/ijerph19020655

Donald Glowinski, Maurizio Mancini, Roddy Cowie, Antonio Camurri, Carlo Chiorri, and Cian Doherty. 2013. The movements made by performers in a skilled quartet: A distinctive pattern, and the function that it serves. *Frontiers in psychology* 4 (11 2013), 841. https://doi.org/10.3389/fpsyg.2013.00841

Lewis R Goldberg. 1992. The development of markers for the Big-Five factor structure. *Psychological assessment* 4, 1 (1992), 26. https://doi.org/10.1037/1040-3590.4.1.26

Martin Gérin-Lajoie, Carol Richards, and Bradford McFadyen. 2005. The Negotiation of Stationary and Moving Obstructions during Walking: Anticipatory Locomotor Adaptations and Preservation of Personal Space. *Motor control* 9 (08 2005), 242–69. https://doi.org/10.1123/mcj.9.3.242

Amy L Hackney, Michael E Cinelli, and James S Frank. 2015. Does the passability of apertures change when walking through human versus pole obstacles? *Acta psychologica* 162 (2015), 62–68. https://doi.org/10.1016/j.actpsy.2015.10.007

Amy L. Hackney, Michael E. Cinelli, and James S. Frank. 2018. Action strategies for walking through multiple, misaligned apertures. *Acta Psychologica* 182 (2018), 100–106. https://doi.org/10.1016/j.actpsy.2017.11.006

Dirk Helbing and Peter Molnar. 1998. Social Force Model for Pedestrian Dynamics. *Physical Review E* 51 (05 1998). https://doi.org/10.1103/PhysRevE.51.4282

Markus Huber, Yi-Huang Su, Melanie Krüger, Katrin Faschian, Stefan Glasauer, and Joachim Hermsdörfer. 2014. Adjustments of speed and path when avoiding collisions with another pedestrian. *PloS one* 9, 2 (2014), e89589. https://doi.org/10.1371/journal.pone.0089589

Jelena Jovancevic-Misic and Mary Hayhoe. 2009. Adaptive Gaze Control in Natural Environments. *Journal of Neuroscience* 29, 19 (2009), 6234–6238. https://doi.org/10.1523/JNEUROSCI.5570-08.2009

Ioannis Karamouzas, Brian Skinner, and Stephen J. Guy. 2014. Universal Power Law Governing Pedestrian Interactions. *Phys. Rev. Lett.* 113 (Dec 2014), 238701. Issue 23. https://doi.org/10.1103/PhysRevLett.113.238701

Robert L. Kosowski and Salih N. Neftci. 2015. Chapter 16 - Correlation as an Asset Class and the Smile. In *Principles of Financial Engineering (Third Edition)* (third

edition ed.), Robert L. Kosowski and Salih N. Neftci (Eds.). Academic Press, San Diego, 545–590. https://doi.org/10.1016/B978-0-12-386968-5.00016-9

Rudolf Laban. 1950. *The mastery of movement on the stage.* Macdonald & Evans.

Myungho Lee, Gerd Bruder, Tobias Höllerer, and Greg Welch. 2018. Effects of Unaugmented Periphery and Vibrotactile Feedback on Proxemics with Virtual Humans in AR. *IEEE Transactions on Visualization and Computer Graphics* 24, 4 (2018), 1525–1534. https://doi.org/10.1109/TVCG.2018.2794074

Peng Li, Chandan Karmakar, John Yearwood, Svetha Venkatesh, Marimuthu Palaniswami, and Changchun Liu. 2018. Detection of epileptic seizure based on entropy analysis of short-term EEG. *PLoS One* 13, 3 (Mar 2018), e0193691. https://doi.org/10.1371/journal.pone.0193691

Richard Lippa. 1998. The Nonverbal Display and Judgment of Extraversion, Masculinity, Femininity, and Gender Diagnosticity: A Lens Model Analysis. *Journal of Research in Personality* 32, 1 (1998), 80–107. https://doi.org/10.1006/jrpe.1997.2189

Sean D. Lynch, Julien Pettré, Julien Bruneau, Richard Kulpa, Armel Crétual, and Anne-Helene Olivier. 2018. Effect of Virtual Human Gaze Behaviour During an Orthogonal Collision Avoidance Walking Task. In *2018 IEEE Conference on Virtual Reality and 3D User Interfaces (VR)*. 136–142. https://doi.org/10.1109/VR.2018.8446180

Tianlu Mao, Ji Wang, Ruoyu Meng, Qinyuan Yan, Shaohua Liu, and Zhaoqi Wang. 2022. A Fusion Crowd Simulation Method: Integrating Data with Dynamics, Personality with Common. *Computer Graphics Forum* 41, 8 (2022), 131–142. https://doi.org/10.1111/cgf.14630 arXiv:https://onlinelibrary.wiley.com/doi/pdf/10.1111/cgf.14630

John D. McCamley, William Denton, Andrew Arnold, Peter C. Raffalt, and Jennifer M. Yentes. 2018. On the Calculation of Sample Entropy Using Continuous and Discrete Human Gait Data. *Entropy* 20, 10 (2018). https://doi.org/10.3390/e20100764

Luis Montesinos, Rossana Castaldo, and Leandro Pecchia. 2018. On the use of approximate entropy and sample entropy with centre of pressure time-series. *Journal of neuroengineering and rehabilitation* 15, 1 (12 Dec 2018), 116. https://doi.org/10.1186/s12984-018-0465-9

Christos Mousas, Dominic Kao, Alexandros Koilias, and Banafsheh Rekabdar. 2021. Evaluating virtual reality locomotion interfaces on collision avoidance task with a virtual character. *Vis. Comput.* 37 (2021), 2823–2839. https://doi.org/10.1007/s00371-021-02202-6

Michael Neff, Nicholas Toothman, Robeson Bowmani, Jean E Fox Tree, and Marilyn A Walker. 2011. Don't scratch! Self-adaptors reflect emotional stability. In *International Workshop on Intelligent Virtual Agents*. Springer, 398–411. https://doi.org/10.1007/978-3-642-23974-8_43

Michael Neff, Yingying Wang, Rob Abbott, and Marilyn Walker. 2010. Evaluating the Effect of Gesture and Language on Personality Perception in Conversational Agents. 222–235. https://doi.org/10.1007/978-3-642-15892-6_24

Michael G. Nelson, Alexandros Koilias, Dominic Kao, and Christos Mousas. 2023. Effects of Speed of a Collocated Virtual Walker and Proximity Toward a Static Virtual Character on Avoidance Movement Behavior. In *2023 IEEE International Symposium on Mixed and Augmented Reality (ISMAR)*. 930–939. https://doi.org/10.1109/ISMAR59233.2023.00109

Haoyu Niu, Jiamin Wei, and YangQuan Chen. 2021. Optimal Randomness for Stochastic Configuration Network (SCN) with Heavy-Tailed Distributions. *Entropy* 23, 1 (2021). https://doi.org/10.3390/e23010056

Anne-Hélène Olivier, Antoine Marin, Armel Crétual, and Julien Pettré. 2012. Minimal predicted distance: A common metric for collision avoidance during pairwise interactions between walkers. *Gait & Posture* 36, 3 (2012), 399–404. https://doi.org/10.1016/j.gaitpost.2012.03.021

Jan Ondrej, Julien Pettre, Anne-Hélène Olivier, and Stéphane Donikian. 2010. A Synthetic-Vision Based Steering Approach for Crowd Simulation. *ACM Transactions on Graphics* 29 (07 2010). https://doi.org/10.1145/1833349.1778860

Yuliya Patotskaya, Ludovic Hoyet, Anne-Hélène Olivier, Julien Pettré, and Katja Zibrek. 2023. Avoiding virtual humans in a constrained environment: Exploration of novel behavioural measures. *Computers and Graphics* 110 (2023), 162–172. https://doi.org/10.1016/j.cag.2023.01.001

Jonathan Perrinet, Anne-Hélène Olivier, and Julien Pettré. 2013. Walk with Me: Interactions in Emotional Walking Situations, a Pilot Study. In *Proceedings of the ACM Symposium on Applied Perception (SAP '13)*. Association for Computing Machinery. https://doi.org/10.1145/2492494.2492507

Iana Podkosova and Hannes Kaufmann. 2018. Co-presence and proxemics in shared walkable virtual environments with mixed colocation *(VRST '18)*. Association for Computing Machinery, New York, NY, USA, Article 21, 11 pages. https://doi.org/10.1145/3281505.3281523

Sofiane Ramdani, Benoît Seigle, Julien Lagarde, Frédéric Bouchara, and Pierre Louis Bernard. 2009. On the use of sample entropy to analyze human postural sway data. *Medical engineering & physics* 31, 8 (2009), 1023–1031. https://doi.org/10.1016/j.medengphy.2009.06.004

Joshua S. Richman and J. Randall Moorman. 2000. Physiological time-series analysis using approximate entropy and sample entropy. *American Journal of Physiology-Heart and Circulatory Physiology* 278, 6 (2000), H2039–H2049.

Alejandro Rios and Nuria Pelechano. 2020. Follower behavior under stress in immersive VR. *Virtual Reality* 24 (12 2020). https://doi.org/10.1007/s10055-020-00428-8

Mélodie Sannier, Stefan Janaqi, Gérard Dray, Pierre Slangen, and Benoît Bardy. 2023. Obstacles shape the way we walk at home. *Frontiers in Computer Science* 5 (12 2023). https://doi.org/10.3389/fcomp.2023.1270520

Jessica C. Selinger, Jennifer L. Hicks, Rachel W. Jackson, Cara M. Wall-Scheffler, Derek Chang, and Scott L. Delp. 2022. Running in the wild: Energetics explain ecological running speeds. *Current Biology* 32, 10 (2022), 2309–2315.e3. https://doi.org/10.1016/j.cub.2022.03.076

Bo Shi, Lili Wang, Chang Yan, Deli Chen, Mulin Liu, and Peng Li. 2019. Nonlinear heart rate variability biomarkers for gastric cancer severity: A pilot study. *Scientific Reports* 9, 1 (2019), 13833. https://doi.org/10.1038/s41598-019-50358-y PMID: 31554842.

Natalie Snyder, Michael Cinelli, Victoria Rapos, Armel Crétual, and Anne-Hélène Olivier. 2022. Collision avoidance strategies between two athlete walkers: Understanding impaired avoidance behaviours in athletes with a previous concussion. *Gait & Posture* 92 (2022), 24–29. https://doi.org/10.1016/j.gaitpost.2021.11.003

Sinan Sonlu, Uğur Güdükbay, and Funda Durupinar. 2021. A Conversational Agent Framework with Multi-modal Personality Expression. *ACM Trans. Graph.* 40, 1, Article 7 (2021), 16 pages. https://doi.org/10.1145/3439795

Wagner Souza Silva, Gayatri Aravind, Samir Sangani, and Anouk Lamontagne. 2018. Healthy young adults implement distinctive avoidance strategies while walking and circumventing virtual human vs. non-human obstacles in a virtual environment. *Gait & Posture* 61 (2018), 294–300. https://doi.org/10.1016/j.gaitpost.2018.01.028

Jur van den Berg, Stephen Guy, Ming Lin, and Dinesh Manocha. 2011. *Reciprocal n-Body Collision Avoidance*. Vol. 70. 3–19. https://doi.org/10.1007/978-3-642-19457-3_1

Cordula Vesper, Robrecht P R D van der Wel, Günther Knoblich, and Natalie Sebanz. 2011. Making oneself predictable: reduced temporal variability facilitates joint action coordination. *Exp Brain Res* 211, 3-4 (2011), 517–30. https://doi.org/10.1007/s00221-011-2706-z

David Wolinski, Stefen Guy, Anne-Hélène Olivier, Ming Lin, Dinesh Manocha, and Julien Pettre. 2014. Parameter Estimation and Comparative Evaluation of Crowd Simulations. *Computer Graphics Forum* 33 (2014). https://doi.org/10.1111/cgf.12328

Pei Xu, Jean-Bernard Hayet, and Ioannis Karamouzas. 2022. Socialvae: Human trajectory prediction using timewise latents. , 511–528 pages. https://doi.org/10.1007/978-3-031-19772-7_30

Chang Yan, Peng Li, Meicheng Yang, Yang Li, Jianqing Li, Hongxing Zhang, and Chengyu Liu. 2022. Entropy Analysis of Heart Rate Variability in Different Sleep Stages. *Entropy (Basel, Switzerland)* 24, 3 (2022), 379. https://doi.org/10.3390/e24030379

Jennifer M Yentes, William Denton, John McCamley, Peter C Raffalt, and Kendra K Schmid. 2018. Effect of parameter selection on entropy calculation for long walking trials. *Gait & Posture* 60 (Feb 2018), 128–134. https://doi.org/10.1016/j.gaitpost.2017.11.023

Wenfeng Yi, Wenhan Wu, Xiaolu Wang, and Xiaoping Zheng. 2023. Modeling the Mutual Anticipation in Human Crowds With Attention Distractions. *IEEE Transactions on Intelligent Transportation Systems* 24, 9 (Sep. 2023), 10108–10117. https://doi.org/10.1109/TITS.2023.3268315

Tairan Yin, Ludovic Hoyet, Marc Christie, Marie-Paule Cani, and Julien Pettré. 2024. With or Without You: Effect of Contextual and Responsive Crowds on VR-based Crowd Motion Capture. *IEEE Transactions on Visualization and Computer Graphics* 30, 5 (2024), 2785–2795. https://doi.org/10.1109/TVCG.2024.3372038

G. Yogarajan, Najah Alsubaie, G. Rajasekaran, T. Revathi, Mohammed S. Alqahtani, Mohamed Abbas, Madshush M. Alshahrani, and Ben Othman Soufiene. 2023. EEG-based epileptic seizure detection using binary dragonfly algorithm and deep neural network. *Scientific Reports* 13, 1 (2023), 17710. https://doi.org/10.1038/s41598-023-44318-w

Lingqi Zeng and Gary M. Bone. 2012. Mobile Robot Navigation for Moving Obstacles with Unpredictable Direction Changes, Including Humans. *Advanced Robotics* 26, 16 (2012), 1841–1862. https://doi.org/10.1080/01691864.2012.703166

A Appendix A

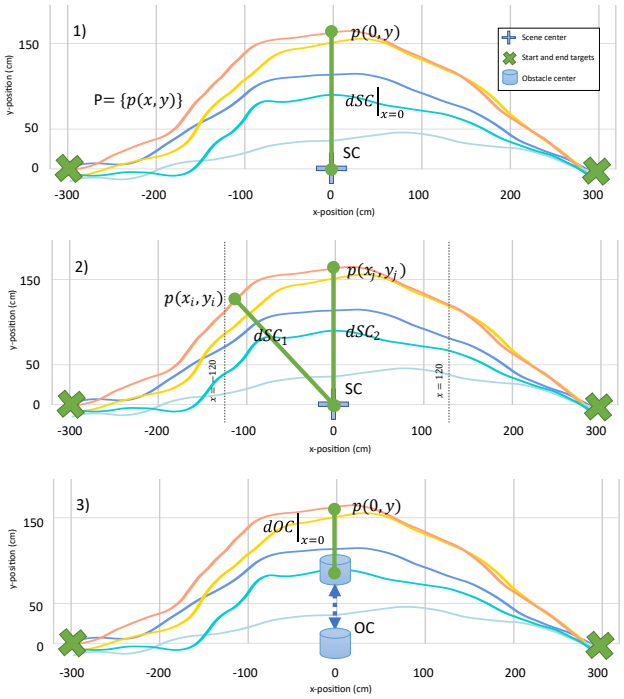

Figure 7: Metrics calculated on participants' trajectories: 1) Side-by-side distance from the center of the scene at $x = 0$: $d_{SC}|_{x=0} = \|p(0,y) - SC\|$; 2) Average distance from the center of the scene: $\tilde{d_{SC}} = \text{avg}(d_{SC_i})|_{i \in \{0,1,\ldots,N\}}$; 3) Side-by-side distance to the center of mass of the obstacle at $x = 0$: $d_{OC}|_{x=0} = \|p(0,y) - OC\|$. Trajectory points $P = \{p(x_i, y_i)\}, i \in \{0, 1, \ldots, N\}$, SC = (0,0) - Scene center coordinate, OC - Obstacle center position.

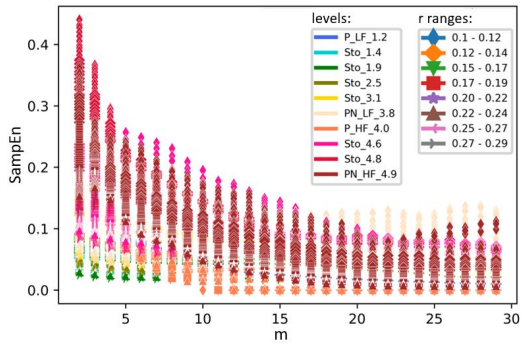

Figure 8: Sample Entropy calculation for various set of parameters m and r for obstacle motion in various conditions.

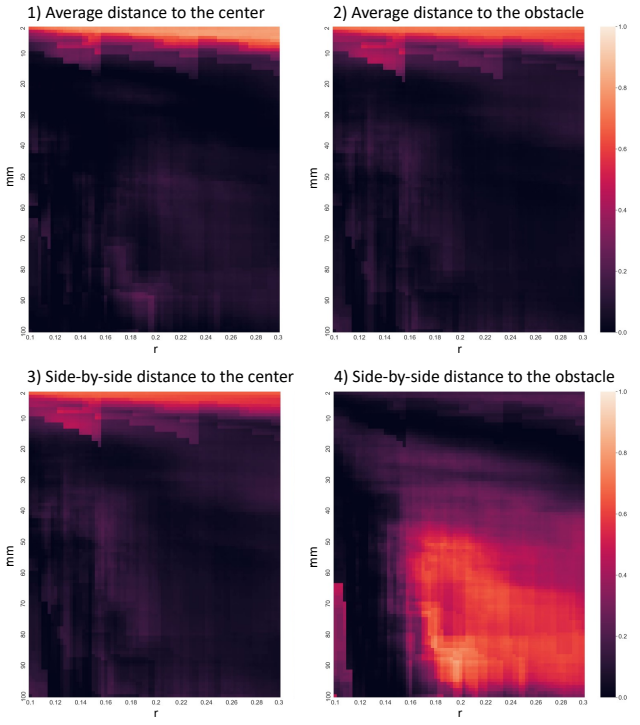

Figure 9: Exploring the relationship between entropy estimations and spatial metrics: A heatmap analysis of linear regression R^2 rates across parameter ranges: 1) Average distance to the center; 2) Average distance to the obstacle; 3) Side-by-side distance to the center; 4) Side-by-side distance to the obstacle.

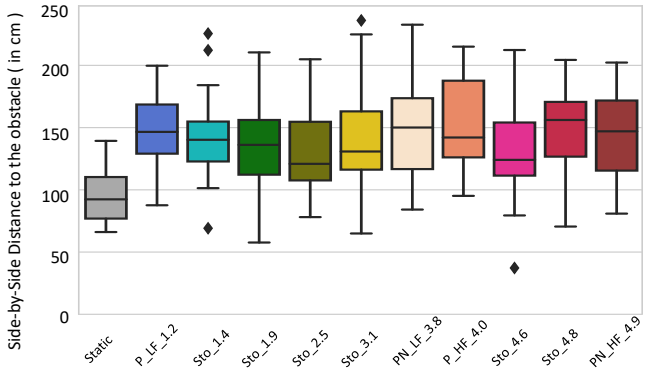

Figure 10: Side-by-Side distance to the obstacle. The significant differences are shown on Table 2.

Table 1: Tukey's post hoc analysis, p-value summary for the metrics related to the center of the scene: 1. Clearance distance; 2. Maximum Lateral Deviation; 3. Side-by-Side Distance; 4. Average Distance. Significant differences (p < 0.05) in red font, absence of significant difference toned in grey.

1. Clearance distance

Conditions	Empty	Static	P_LF_1.2	Sto_1.4	Sto_1.9	Sto_2.5	Sto_3.1	PN_LF_3.8	P_HF_4.0	Sto_4.6	Sto_4.8
Static	.001										
P_LF_1.2	.001	1.000									
Sto_1.4	.001	.001	0.040								
Sto_1.9	.001	.001	0.052	1.000							
Sto_2.5	.001	.001	0.006	0.567	0.981						
Sto_3.1	.001	.001	0.001	0.160	0.557	0.857					
PN_LF_3.8	.001	.001	0.002	0.999	1.000	0.999	0.852				
P_HF_4.0	.001	.001	.001	0.014	0.007	0.121	0.653	0.036			
Sto_4.6	.001	.001	0.006	0.357	0.538	0.760	1.000	0.864	0.914		
Sto_4.8	.001	.001	.001	0.006	0.008	0.034	0.122	.001	0.862	0.410	
PN_HF_4.9	.001	.001	.001	0.020	0.004	0.055	0.425	0.012	1.000	0.563	0.929

2. Maximum lateral deviation

Conditions	Empty	Static	P_LF_1.2	Sto_1.4	Sto_1.9	Sto_2.5	Sto_3.1	PN_LF_3.8	P_HF_4.0	Sto_4.6	Sto_4.8
Static	.001										
P_LF_1.2	.001	0.440									
Sto_1.4	.001	.001	0.378								
Sto_1.9	.001	.001	0.610	1.000							
Sto_2.5	.001	.001	0.097	0.892	0.308						
Sto_3.1	.001	.001	0.007	0.004	0.017	0.281					
PN_LF_3.8	.001	.001	0.014	1.000	0.931	1.000	0.502				
P_HF_4.0	.001	.001	.001	0.008	0.001	0.125	0.784	0.017			
Sto_4.6	.001	.001	0.009	0.019	0.007	0.300	0.969	0.304	0.998		
Sto_4.8	.001	.001	.001	0.004	.001	0.026	0.201	0.001	0.991	0.815	
PN_HF_4.9	.001	.001	.001	0.021	0.009	0.189	0.838	0.023	1.000	1.000	0.930

3. Side-by-side distance

Conditions	Empty	Static	P_LF_1.2	Sto_1.4	Sto_1.9	Sto_2.5	Sto_3.1	PN_LF_3.8	P_HF_4.0	Sto_4.6	Sto_4.8
Static	.001										
P_LF_1.2	.001	0.988									
Sto_1.4	.001	.001	0.052								
Sto_1.9	.001	.001	0.101	1.000							
Sto_2.5	.001	.001	0.008	0.424	0.629						
Sto_3.1	.001	.001	0.003	0.034	0.140	0.888					
PN_LF_3.8	.001	.001	0.008	1.000	1.000	0.982	0.644				
P_HF_4.0	.001	.001	.001	0.008	0.001	0.232	0.769	0.024			
Sto_4.6	.001	.001	0.006	0.044	0.014	0.410	0.901	0.340	1.000		
Sto_4.8	.001	.001	.001	0.002	.001	0.036	0.084	.001	0.883	0.819	
PN_HF_4.9	.001	.001	.001	0.012	0.002	0.128	0.448	0.009	1.000	0.998	0.752

4. Average distance

Conditions	Empty	Static	P_LF_1.2	Sto_1.4	Sto_1.9	Sto_2.5	Sto_3.1	PN_LF_3.8	P_HF_4.0	Sto_4.6	Sto_4.8
Static	.001										
P_LF_1.2	.001	0.901									
Sto_1.4	.001	.001	0.084								
Sto_1.9	.001	.001	0.158	1.000							
Sto_2.5	.001	.001	0.017	0.670	0.826						
Sto_3.1	.001	.001	0.003	0.070	0.214	0.448					
PN_LF_3.8	.001	.001	0.002	0.999	1.000	1.000	0.819				
P_HF_4.0	.001	.001	.001	0.005	0.001	0.050	0.539	0.010			
Sto_4.6	.001	.001	0.008	0.108	0.060	0.347	0.998	0.639	0.960		
Sto_4.8	.001	.001	.001	0.002	.001	0.014	0.101	.001	0.870	0.569	
PN_HF_4.9	.001	.001	.001	0.027	0.008	0.078	0.608	0.016	1.000	0.951	0.788

Table 2: Tukey's post hoc analysis of Side-by-side distance from the participant to center of mass of the moving obstacle: p-values summary highlighting significant differences (p < 0.05) in red font, absence of significant difference toned in grey.

Conditions	Empty	Static	P_LF_1.2	Sto_1.4	Sto_1.9	Sto_2.5	Sto_3.1	PN_LF_3.8	P_HF_4.0	Sto_4.6	Sto_4.8
Static	.001										
P_LF_1.2	.001	0.985									
Sto_1.4	.001	.001	0.048								
Sto_1.9	.001	.001	0.111	1.000							
Sto_2.5	.001	.001	0.007	0.357	0.405						
Sto_3.1	.001	.001	0.003	0.036	0.119	0.880					
PN_LF_3.8	.001	.001	0.006	1.000	1.000	0.984	0.644				
P_HF_4.0	.001	.001	.001	0.014	0.002	0.378	0.936	0.040			
Sto_4.6	.001	.001	0.005	0.039	0.006	0.444	0.943	0.367	1.000		
Sto_4.8	.001	.001	.001	0.002	.001	0.046	0.137	.001	0.781	0.842	
PN_HF_4.9	.001	.001	.001	0.012	0.001	0.141	0.529	0.010	1.000	0.998	0.802

Table 3: Comparison of side-by-side distances to the scene center: Tukey's post hoc p-values summary highlighting significant differences (p < 0.05) in red font. Table 1 represents all participants, 2 - "avoiders" and 3 - "anticipators".

1. All participants

Conditions	Static	P_LF_1.2	Sto_1.4	Sto_1.9	Sto_2.5	Sto_3.1	PN_LF_3.8	P_HF_4.0	Sto_4.6	Sto_4.8	PN_HF_4.9
P_LF_1.2	0.988		0.052	0.101	0.008	0.003	0.008	< .001	0.006	< .001	< .001
Sto_1.4	< .001	0.052		1.000	0.424	0.034	1.000	0.008	0.044	0.002	0.012
Sto_1.9	< .001	0.101	1.000		0.629	0.140	1.000	0.001	0.014	< .001	0.002
Sto_2.5	< .001	0.008	0.424	0.629		0.888	0.982	0.232	0.410	0.036	0.128
Sto_3.1	< .001	0.003	0.034	0.140	0.888		0.644	0.769	0.901	0.084	0.448
PN_LF_3.8	< .001	0.008	1.000	1.000	0.982	0.644		0.024	0.340	< .001	0.009
P_HF_4.0	< .001	< .001	0.008	0.001	0.232	0.769	0.024		1.000	0.883	1.000
Sto_4.6	< .001	0.006	0.044	0.014	0.410	0.901	0.340	1.000		0.819	0.998
Sto_4.8	< .001	< .001	0.002	< .001	0.036	0.084	< .001	0.883	0.819		0.752
PN_HF_4.9	< .001	< .001	0.012	0.002	0.128	0.448	0.009	1.000	0.998	0.752	

2. Avoiders

Conditions	Static	P_LF_1.2	Sto_1.4	Sto_1.9	Sto_2.5	Sto_3.1	PN_LF_3.8	P_HF_4.0	Sto_4.6	Sto_4.8	PN_HF_4.9
P_LF_1.2	0.862		0.269	0.194	0.033	0.017	0.040	.001	0.033	.001	.001
Sto_1.4	.001	0.269		1.000	0.828	0.475	0.858	0.015	0.224	0.001	0.024
Sto_1.9	.001	0.194	1.000		0.963	0.456	0.999	0.018	0.082	.001	0.008
Sto_2.5	.001	0.033	0.828	0.963		0.969	1.000	0.312	0.833	0.058	0.117
Sto_3.1	.001	0.017	0.475	0.456	0.969		0.998	0.823	0.995	0.158	0.373
PN_LF_3.8	.001	0.040	0.858	0.999	1.000	0.998		0.249	0.942	0.004	0.118
P_HF_4.0	.001	.001	0.015	0.018	0.312	0.823	0.249		0.998	0.881	1.000
Sto_4.6	.001	0.033	0.224	0.082	0.833	0.995	0.942	0.998		0.630	0.863
Sto_4.8	.001	.001	0.001	.001	0.058	0.158	0.004	0.881	0.630		0.963
PN_HF_4.9	.001	.001	0.024	0.008	0.117	0.373	0.118	1.000	0.863	0.963	

3. Anticipators

Conditions	Static	P_LF_1.2	Sto_1.4	Sto_1.9	Sto_2.5	Sto_3.1	PN_LF_3.8	P_HF_4.0	Sto_4.6	Sto_4.8	PN_HF_4.9
P_LF_1.2	0.557		.001	0.002	.001	.001	.001	.001	.001	.001	.001
Sto_1.4	.001	.001		0.107	0.143	0.057	0.825	0.212	.001	0.020	0.079
Sto_1.9	0.013	0.002	0.107		0.002	.001	0.164	0.005	.001	.001	.001
Sto_2.5	.001	.001	0.143	0.002		0.659	0.092	0.825	0.041	0.378	0.769
Sto_3.1	.001	.001	0.057	.001	0.659		0.034	0.508	0.107	0.659	0.883
PN_LF_3.8	.001	.001	0.825	0.164	0.092	0.034		0.143	.001	0.011	0.048
P_HF_4.0	.001	.001	0.212	0.005	0.825	0.508	0.143		0.024	0.271	0.607
Sto_4.6	.001	.001	.001	.001	0.041	0.107	.001	0.024		0.240	0.079
Sto_4.8	.001	.001	0.020	.001	0.378	0.659	0.011	0.271	0.240		0.557
PN_HF_4.9	.001	.001	0.079	.001	0.769	0.883	0.048	0.607	0.079	0.557	